S. cerevisiae Cwc15p Tunes the Spliceosome Active Site for 5' Splice Site Cleavage

Natalie J. Zeps[1], Giovanni Balice[1], Zach Freedman[1], Sierra Jones[2], Dennis Halterman[2,3], and Aaron A. Hoskins[1,4*]

[1]Department of Biochemistry, University of Wisconsin-Madison, Madison, WI 53706
[2]Department of Plant Pathology, University of Wisconsin-Madison, Madison, WI 53706
[3]USDA-ARS Vegetable Crops Research Unit, Madison, WI 53706
[4]Department of Chemistry, University of Wisconsin-Madison, Madison, WI 53706

***CORRESPONDING AUTHOR:**
Aaron A. Hoskins, ahoskins@wisc.edu

ORCID:
Natalie J. Zeps, 0009-0001-0625-404X
Dennis Halterman, 0000-0002-2428-9393
Aaron A. Hoskins, 0000-0002-9777-519X

Running Title: Roles of Cwc15p in Pre-mRNA Splicing

KEYWORDS: pre-mRNA, splicing, yeast, spliceosome, RNA, *S. cerevisiae*

ABSTRACT (250 words)

Pre-mRNA splicing is an essential step in eukaryotic gene expression during which spliceosomes remove introns from nascent RNAs while ligating the adjacent exons. Spliceosomes are cellular nanomachines composed of five small nuclear (snRNA) components and dozens of proteins, most of which are highly conserved. Despite the high conservation of many splicing factors between *S. cerevisiae* and *H. sapiens*, several protein components of the *S. cerevisiae* spliceosome are not essential for growth under normal laboratory conditions. This is particularly surprising for nonessential factors whose conserved domains contact the spliceosome's catalytic core. Uncovering a function for these splicing factors can be challenging since they are not required for viability, may engage in functionally redundant interactions, and may display only weak phenotypes in the absence of secondary mutations in other spliceosome components. One such nonessential factor is the Cwc15 protein. Cwc15's highly conserved N-terminus directly contacts the U2/U6 di-snRNA within the spliceosome catalytic core; yet its precise role in splicing has not been defined in any organism. In this work, we use molecular genetics in *S. cerevisiae* combined with splicing reporter assays to study Cwc15p function. We propose that Cwc15p not only promotes active site stability during 5' splice site cleavage but also impacts structural transitions into and out of this spliceosome conformation. This function may be critical for splicing in *S. cerevisiae* under nonoptimal conditions, facilitating use of weak or alternate splice sites, and could have implications for proofreading of spliceosome active site formation.

47 **Graphical Abstract**

48 Created in BioRender. Hoskins, A. (2026) https://BioRender.com/9nrbm6r

Article Summary (100 word)

Pre-mRNA splicing is carried out by large macromolecular machines called spliceosomes which are composed of several snRNAs and dozens of proteins. Despite decades of study, the functions of many splicing factors such as *S. cerevisiae* Cwc15p remain unknown. Cwc15p is highly conserved among eukaryotes and directly contacts the spliceosome catalytic core. Here, we have used genetic and splicing reporter assays to study the function of Cwc15p during splicing *in vivo*. We propose that Cwc15p both stabilizes the spliceosome active site during 5' splice site cleavage and impacts remodeling of that site.

INTRODUCTION

In eukaryotes, nuclear DNA genes frequently contain introns which must be removed from precursor mRNA (pre-mRNA) transcripts concomitant with ligation of the flanking exons for gene expression (**Fig. 1A**). This process, called pre-mRNA splicing, is carried out by a large macromolecular machine called the spliceosome. Spliceosomes assemble around introns from uridine-rich small nuclear RNAs (the U snRNAs; U1, U2, U4, U5, and U6) and dozens of protein components. The snRNAs and many proteins associate with introns in pre-assembled complexes called small nuclear ribonucleoproteins (snRNPs). Other proteins also join spliceosomes in either multi-subunit complexes lacking RNA components [such as the Prp19-containing complex or Nineteen Complex (NTC)] or as individual units. The processes of spliceosome assembly and correct identification of introns are complex and involve numerous ATP-dependent and -independent stages (Plaschka et al. 2019; Kastner et al. 2019).

Once assembled, spliceosomes contain RNA active sites composed of the U2 and U6 snRNAs, the pre-mRNA substrate, and metal ions (Fica et al. 2013; Senn et al. 2024; Yan et al. 2019). Despite being ribozymes at their catalytic heart, the RNAs require numerous proteins to scaffold and arrange them into the catalytic conformations needed for 5' splice site (5'SS) cleavage (1st chemical step of splicing) and exon ligation (2nd step). While some of these proteins, such as Prp8p (Grainger and Beggs 2005), are essential components of the splicing machinery, a number of other protein splicing factors are not required (or at least not under certain conditions). In particular, the NTC and its related complexes contain many proteins that are non-essential in *Saccharomyces cerevisiae* (yeast) for growth and pre-mRNA splicing under laboratory conditions (Hogg et al. 2010).

82 For several of these proteins, their non-essentiality is surprising given their locations near
83 the spliceosome active site and contacts with critical protein and RNA components in
84 cryo-EM structures. Network analysis of these structures suggested that non-essentiality
85 may be due to redundancy in splicing factor interactions—non-essential factors make
86 fewer unique interactions compared with essential factors (Kaur et al. 2022). This implies
87 that they primarily function in *S. cerevisiae* to fine-tune splicing reactions under certain
88 conditions or on certain substrates.

89 One nonessential component is yeast Cwc15p. Cwc15p is a small, 20 kDa protein
90 that was identified as complexed with Cef1 (or cdc5 in *Schizosaccharomyces pombe*) by
91 mass spectrometry of purified splicing factor complexes (Ohi et al. 2002). Despite being
92 non-essential in *S. cerevisiae*, Cwc15p is highly conserved with homologs present
93 throughout eukaryotes including in humans and plants (Ohi et al. 2002) (**Fig. S1**). Cwc15p
94 homologs are essential in *S. pombe* (Ohi et al. 2002), *Arabidopsis* (Slane et al. 2020),
95 and *Bos taurus* (Sonstegard et al. 2013). This suggests that organisms with more complex
96 splicing regulatory mechanisms, intron composition, and/or machineries than *S.*
97 *cerevisiae* (Sales-Lee et al. 2021) require Cwc15p for proper spliceosome function.

98 No detailed biochemical or molecular genetics work has been reported for analysis
99 of Cwc15p's function during pre-mRNA splicing. Cryo-EM structures of catalytic-stage
100 spliceosomes from a variety of organisms all show that Cwc15p lacks appreciable
101 secondary structure and threads its way throughout the spliceosome (**Fig. 1B**). Cwc15p's
102 highly conserved N-terminus (**Fig. S1**) inserts directly into the catalytic core of the
103 spliceosome, contacting the back of the catalytic U2/U6 snRNA duplex opposite of the
104 face on which catalytically essential metal ions are bound (**Fig. 1B**, boxed region). Large

105 portions of the remainder of Cwc15p are unresolved in available cryo-EM structures;
106 however, a tryptophan in a conserved region near the C-terminus (**Fig. S1**) is visible and
107 interacts with a hydrophobic pocket on Prp8p (the large protein responsible for scaffolding
108 the catalytic RNAs). Given these interactions with critical components of the spliceosome,
109 it is likely that Cwc15p influences pre-mRNA splicing despite being non-essential in *S.*
110 *cerevisiae*. In support of this, *S. cerevisiae cwc15*Δ is synthetically lethal with the *prp19-*
111 *1* allele (Ohi et al. 2002), and in *S. pombe*, the *fsm32* mutant allele of *CWF15* (the *S.*
112 *pombe* homolog of *CWC15*) results in intron retention and splicing defects of the MCS2
113 transcript (Hoyos-Manchado et al. 2017). Additional evidence comes from studies of plant
114 Cwc15 proteins. The *Arabidopsis cwc15-1* allele causes splicing defects *in vivo*, although
115 these were not extensively characterized (Slane et al. 2020), and *S. tuberosum* (potato)
116 Cwc15p was recently found to be the target of the pathogen *Phytophthora infestans*
117 effector protein IPI-O1 (Sun et al. 2024). This interaction results in a change in splicing of
118 an immunity gene in potato, resulting in pathogen resistance.

119 Here, we use yeast molecular genetics to probe the function of Cwc15p during pre-
120 mRNA splicing. By testing genetic interactions between *cwc15*Δ and splicing factors and
121 using *in vivo* splicing reporter assays, we propose that Cwc15p stabilizes the active site
122 during 1st step catalysis while also facilitating its remodeling before and after this step.

123 **MATERIALS AND METHODS:**

124 <u>Yeast strain and plasmid construction</u>

125 The *CWC15* gene was deleted from yeast strains by replacement with a
126 hygromycin resistance cassette (HygR) through homologous recombination (Goldstein
127 and McCusker 1999). Gene deletions were confirmed by PCR.

128 Mutant *CWC15* and *SNR6* plasmids were constructed either by site-directed
129 mutagenesis using inverse PCR (Silva et al. 2023) or by purchasing plasmids containing
130 the appropriate DNAs from GENEWIZ (South Plainfield, NJ USA) or Genscript
131 (Pennington, NJ USA). All plasmids were sequenced before use by Sanger or whole-
132 plasmid next-generation DNA sequencing (Functional Biosciences; Madison, WI USA).
133 Yeast growth and transformation were carried out using standard protocols and media
134 (Guthrie et al. 1991). Yeast strains and plasmids are listed in **Sup. Tables S1** and **S2**,
135 respectively.

136 Yeast growth assays at various temperatures

137 Yeast cultures were grown overnight in liquid culture to saturation and then
138 adjusted to an OD_{600} of 0.5 in 10% (v/v) glycerol. Three consecutive 1:10 serial dilutions
139 were performed by transferring 100 µL of culture into 900 µL of diluent, resulting in final
140 dilutions of 1:1, 1:10, 1:100, and 1:1000. Diluted cultures were then spotted onto plates
141 and incubated at 16°C, 23°C, 30°C, or 37°C before imaging with an ImageQuant™ LAS
142 4000 imaging system (GE Healthcare/Cytiva). Assays were performed in at least
143 triplicate.

144 ACT1-CUP1 assays

145 Yeast strains transformed with ACT1–CUP1 reporter plasmids were cultured in -
146 Leu dropout (DO) media. Diluted cultures (OD_{600} = 0.5) were spotted onto -Leu DO plates
147 supplemented with 0–2.5 mM $CuSO_4$ (Lesser and Guthrie 1993; Carrocci et al. 2018) and
148 incubated at 30°C for 3 days before imaging.

149 **RESULTS**

150 Genetic Interactions between *CWC15* and Spliceosomal ATPases

151 To assay Cwc15p function, we first deleted the *CWC15* gene from *S. cerevisiae*
152 and studied yeast growth at various temperatures (**Fig. 1C**). Consistent with a recent
153 report by Henke-Schulz and colleagues (Henke-Schulz et al. 2024), we observed that
154 *cwc15*Δ yeast had no observable growth defect at 16, 23, or 30°C on YPD plates but grew
155 more slowly and were heat sensitive (temperature sensitive or *ts*) at 37°C. (We note that
156 the strength of the *ts* phenotype is strain dependent with some strains growing more
157 robustly at 37°C, *c.f.* **Figs. 1C** vs. **5E**, for example).

158 Given Cwc15p's location proximal to the spliceosome active site, we hypothesized
159 that genetic interactions may exist between *cwc15*Δ and the DEAH-box ATPases
160 responsible for remodeling the spliceosome during formation or disruption of the catalytic
161 center. We tested genetic interactions between *cwc15*Δ and *PRP2*, *PRP16*, and *PRP22*
162 (**Fig. 2A**). Prp2p is responsible for releasing U2 snRNP proteins from the branch site
163 (BS)/U2 snRNA duplex and proofreading the catalytic core during the final stages of active
164 site assembly (Schmitzova et al. 2023; Lardelli et al. 2010; Wlodaver and Staley 2014).
165 Prp16p is responsible for releasing proteins from the spliceosome required for 5'SS
166 cleavage in order to facilitate active site reorganization and for proofreading the 1st step
167 (Koodathingal et al. 2010; Chung et al. 2023; Tseng et al. 2011). Prp22p is responsible
168 for proofreading exon ligation as well as releasing the mRNA product and proteins needed
169 during the 2nd step (Mayas et al. 2006; Company et al. 1991; Chung et al. 2025).

170 The Prp2p^{Q548N} mutation is cold sensitive (*cs*), inhibits splicing *in vivo*, and likely
171 inhibits ATP binding or hydrolysis by the enzyme (Wlodaver and Staley 2014). Splicing
172 inhibition arises due to difficulties in disruption of U2/U6 di-snRNA interactions needed for
173 the final stages of catalytic site folding. Destabilizing mutations in these snRNAs or other

174 splicing factors involved in activation can suppress the *cs* phenotype while stabilizing
175 mutations can do the opposite (Wlodaver and Staley 2014; Carrocci et al. 2017; van der
176 Feltz et al. 2021). When we combined Prp2p^{Q548N} with *cwc15*Δ, we observed that yeast
177 were synthetic sick at 30ºC and synthetic lethal at 16, 23, and 37ºC (**Fig. 2B**). This
178 indicates that Cwc15p functions during spliceosome active site formation and that loss of
179 Cwc15p is detrimental if aberrant Prp2p activity is present. This phenotype could arise
180 due to Cwc15p functioning to destabilize the U2/U6 di-snRNA during activation and/or
181 stabilizing the product of Prp2p remodeling (*i.e.,* the 1st-step active site of the
182 spliceosome). We favor the latter mechanism because it may provide a function for the
183 highly conserved Cwc15p N-terminus (see Discussion).

184 We then tested genetic interactions with mutants in Prp16p and Prp22p.
185 Prp16p^{R686I} is *cs* at 16ºC and *ts* at 37ºC, and at the latter temperature can be suppressed
186 by the *prp8-156* allele which favors the exon ligation conformation of the active site (Query
187 and Konarska 2004; Hotz and Schwer 1998). Similarly, the *cs* phenotype can be
188 suppressed by *ecm2*Δ, which eliminates a nonessential splicing factor that makes
189 stabilizing interactions in the 5'SS conformation (van der Feltz et al. 2021). Prp22p^{T637A}
190 decouples ATP hydrolysis from RNA unwinding and causes a *cs* phenotype *in vivo*
191 (Schwer and Meszaros 2000). Prp22p^{T637A} is also synthetic lethal at certain temperatures
192 with loss of the 2nd-step splicing factor Fyv6p or alleles of *CEF1* that disrupt exon ligation
193 (Lipinski et al. 2023; Query and Konarska 2012). Combined, these observations support
194 a model in which Prp16p and Prp22p promote exit from the 1st and 2nd-step conformations
195 of the active site, respectively; Prp16p^{R686I} and Prp22p^{T637A} inhibit these transitions; and

196 that the effects of these mutations can be suppressed (or exacerbated) by changes in the
197 relative stabilities of the active site conformations (Liu et al. 2007).

198 Genetic interactions were less pronounced with Prp16p^{R686I} and Prp22p^{T637A}
199 mutants relative to Prp2p^{Q548N}. Loss of Cwc15p in cells expressing Prp16p^{R686I} caused a
200 slight suppression of the *cs* phenotype; although, Prp16p^{R686I}/*cwc15*Δ cells still grew
201 poorly at 16°C (**Fig. 2B**). At 37°C, Prp16p wild type (Prp16p^{WT})/*cwc15*Δ also grew poorly
202 while Prp16p^{R686I}/*cwc15*Δ cells did not grow. Similarly, the *cwc15*Δ *ts* phenotype was
203 exacerbated by Prp22p^{T637A} (**Fig. 2B**). However, the *cs* phenotype due to Prp22p^{T637A} was
204 not suppressed by *cwc15*Δ. As with Prp2p, these results with Prp16p and Prp22p are
205 consistent with Cwc15p impacting spliceosome active site stability and in ways that
206 change the ATPase-dependence of transitions between conformations or formation of
207 transient, intermediate structures (Eysmont et al. 2019).

208 Genetic Interactions Between *CWC15, PRP8, and SNR6*

209 As mentioned above, different alleles or mutants of yeast Prp8p have been shown
210 to influence pre-mRNA splicing by promoting the formation or stability of the active site
211 for a given step at the expense of the other (*e.g.,* promoting the 1st step reaction but
212 inhibiting the 2nd step, **Fig. 3A**) (Liu et al. 2007). Given our results with the ATPases (**Fig.
213 2**), we next tested genetic interactions between *PRP8* 1st- or 2nd-step alleles and *cwc15*Δ.

214 We expressed Prp8p mutants (Prp8p^{P986T}, 2nd step allele (*prp8-161*); Prp8p^{R1753K},
215 1st-step allele; and Prp8p^{E1960K}, 1st-step allele (*prp8-101*)) (Liu et al. 2007) in the presence
216 of *CWC15* or in a deletion background (**Fig. 3B**). Deletion of *CWC15* was able to suppress
217 the *ts* phenotype at 37°C for both 1st-step alleles (Prp8p^{R1753K} and Prp8p^{E1960K}). In
218 addition, yeast containing the 2nd-step allele Prp8p^{P986T} grew slightly better in the absence

219 of Cwc15p than in its presence at 37°C. Loss of *CWC15* was also able to suppress the
220 *cs* phenotype of the Prp8p^{E1960K} mutant at 16°C. When 1st- and 2nd-step alleles are
221 combined in the same *PRP8* gene, they can cancel each other's effects (Liu et al. 2007).
222 While the addition of the Prp8p^{P986T} mutation restored growth at 37°C for Prp8p^{R1753K} in
223 the presence of Cwc15p, this effect was lost and yeast became sicker at all temperatures
224 when *CWC15* was deleted.

225 These results are consistent with a role for Cwc15p in stabilizing the 1st step
226 conformation of the spliceosome active site at a stage that acts in concert with Prp8p 1st-
227 step alleles. When the active site is destabilized due to loss of Cwc15p, the impact of
228 *PRP8* 1st-step alleles is weakened and growth is restored at 37°C. Cwc15p could also
229 have some additional function during the 2nd-step or at other stages given the weaker
230 effects seen with the Prp8^{P986T} mutant and the synthetic *cs* phenotype observed with
231 Prp8p$^{P986T+R1753K}$ in *cwc15*Δ cells.

232 Since mutations in the U6 snRNA gene (*SNR6*) can also change the relative
233 efficiencies of the 1st and 2nd steps splicing, we then tested whether U6 mutants that favor
234 (U57A, U70A, A79U) or disfavor (U57C, G63C, U65A) the transition between the 1st and
235 2nd step also have genetic interactions with *cwc15*Δ (Liu et al. 2007; Query and Konarska
236 2004; Eysmont et al. 2019). These mutations also span different regions of the U6 snRNA
237 including the upper and lower telestem (U70A, A79U and G63C, U65A; respectively) and
238 the U2/U6 di-snRNA (U57A, U57C). The lower telestem is proposed to play a key role in
239 formation of a transitional spliceosome structure between active conformations (Eysmont
240 et al. 2019).

241 In this case, we see the strongest genetic interactions between U6-U57C and
242 *cwc15*Δ, which are synthetic lethal at 37°C and cause poor growth at 16°C relative to cells
243 with *CWC15* (**Fig. 3C**). U57C is thought to stabilize the 1st step conformation of the
244 spliceosome or disfavor transitions away from this state (Liu et al. 2007; Eysmont et al.
245 2019; Wlodaver and Staley 2014). We favor an interpretation that Cwc15p facilitates the
246 1st-to-2nd step transition and loss of Cwc15p in combination with U6-U57C makes this
247 transition more difficult. In combination with results from Prp8p and the ATPases, one
248 model for Cwc15p function could be that it both stabilizes the active site during 5'SS
249 cleavage and facilitates rearrangement of the active site at stages preceding or following
250 catalysis. The latter activity could occur by destabilization of the active site conformation
251 at those times and/or by impacting the formation or stability of structures that form during
252 remodeling.

253 Impact of *CWC15* Deletion on Yeast Growth with ACT1-CUP1 Splicing Reporters

254 To further assess Cwc15p's role in pre-mRNA splicing, we used the *in vivo* ACT1-
255 CUP1 splicing reporter assay (Lesser and Guthrie 1993). In this assay, copper-sensitive
256 yeast are transformed with a plasmid encoding a gene for the Cup1p copper resistance
257 protein with derivatives of the *ACT1* intron inserted into its coding sequence (**Fig. 4A**).
258 They are then grown on plates containing increasing concentrations of Cu^{2+}. Growth in
259 the presence of copper requires splicing of the *ACT1-CUP1* pre-mRNA and expression
260 of the Cup1p protein. The degree of resistance of the yeast to copper correlates with the
261 extent of splicing.

262 Using the WT ACT1-CUP1 reporter, which contains consensus yeast splice sites,
263 we observed no change in resistance to copper between WT and *cwc15*Δ strains and

264 both readily grew on plates containing the maximal copper concentration (2.5 mM) (**Fig.**
265 **4B**). This indicates a high splicing efficiency for the ACT1-CUP1 reporter even when
266 Cwc15p is absent under these conditions. This likely explains, at least in part, the lack of
267 a significant growth phenotype at 30°C for the deletion strain since the majority of yeast
268 introns contain consensus splice sites.

269 We next tested growth of yeast containing reporters with a variety of substitutions
270 at the 5' or 3'SS or BS sequence (**Fig. 4A**, **B**). In these cases, we saw changes in copper
271 tolerances for the WT *vs. cwc15*Δ strains for particular variants. For the 5'SS, we observed
272 slight increases in tolerance for G+1 substitutions (G1A, G1C) and a reduction in
273 tolerance for the U2C reporter. For substitutions at the branch site, we observed
274 reductions in tolerance for both the BS-C and BS-G substitutions as well as for a C260A
275 substitution at the 3' flanking position. We did not observe any changes in copper
276 tolerance for yeast with substitutions at the -3 (gAG) and -2 (UuG) positions of the 3'SS.

277 Overall, the results show that loss of *CWC15* impacts the 1st-step splicing reaction
278 and changes copper tolerances observed with reporters that are limiting for 5'SS
279 cleavage: G1A, G1C, BS-C, and C260A. In contrast, we did not observe changes in
280 tolerance for most reporters limiting for exon ligation: U2A, A3C, gAG, and UuG with the
281 exception of BS-G (Liu et al. 2007). Despite impacting growth due to the variant ACT1-
282 CUP1 reporters, the *cwc15*Δ allele does not behave identically to characterized Prp8 1st
283 or 2nd-step alleles since we observe changes at the G+1 position and do not observe
284 other characteristic changes in growth (*e.g.*, decreased copper tolerance for the A3C
285 reporter for 1st-step alleles and increases in copper tolerances for gAG and UuG reporters
286 for 2nd-step alleles) (Liu et al. 2007; Query and Konarska 2004).

287 Genes Encoding Mutant Cwc15 Proteins Can Rescue Yeast Growth

288 We next tested if conserved regions of Cwc15p were essential for rescuing the *ts*
289 phenotype (**Fig. 1C**). The most highly conserved region in Cwc15p is the N-terminus,
290 which inserts into the spliceosome active site between the U2 and U6 snRNAs and
291 contacts many key splicing factors (**Fig. 5A**, **B**). In a cryo-EM structure of the *S. cerevisiae*
292 spliced product spliceosome (P complex), Cwc15p residues Thr2 and Thr3 form hydrogen
293 bonding interactions with U6 snRNA nucleotides C84 and C85 (Senn et al. 2024). Arg6
294 also forms a cation-π stacking interaction with U2 snRNA G20, and Gly14 closely packs
295 into an interface with Prp46p. Additionally, conservation of Pro7 may be due to limiting
296 flexibility of the N-terminus and facilitating its threading through a small channel formed
297 between U2 snRNA G20/G21 and U6 snRNA A62/G63. We hypothesized that these
298 interactions could be disrupted using T2V/T3V substitutions which replace hydrophilic
299 with hydrophobic side chains that cannot hydrogen bond to U6 nucleotides, an
300 H5A/R6A/P7A/Q8A quadruple mutant (AAAA) that eliminates the cation-π interaction with
301 U2 and increases flexibility at position 7, or by introducing a side chain at the interface
302 with Prp46p with a G14A mutation.

303 In addition to the N-terminus, Cwc15 proteins also contain a conserved tryptophan
304 residue located in the C-terminal half. This tryptophan is flanked by charged amino acids
305 and fits into a hydrophobic pocket found on the Prp8 protein in the reverse transcriptase-
306 like domain (**Fig. 5C, D**). Therefore, we also made Cwc15p mutants in which the
307 tryptophan (Trp127) was substituted with a differently-shaped and charged residue
308 (glutamate or lysine), which would be less favorable to bury within this pocket.

309 We transformed a *cwc15*Δ yeast strain with TRP1/CEN plasmids expressing either
310 WT Cwc15p or mutants expressed from the endogenous promoter and selected for
311 growth on -trp plates. None of the mutants caused any growth defect at 30°C (not shown).
312 We then assayed growth at a higher temperature to test for rescue of the *ts* phenotype.
313 In these experiments, we found that the *ts* phenotype was more apparent at 39°C than
314 37°C. Yeast lacking Cwc15p and transformed with an empty pRS414 plasmid grew more
315 slowly than those containing a plasmid that expressed WT Cwc15p (**Fig. 5E**). This
316 indicates that a plasmid-borne copy of the WT *CWC15* gene can rescue the *ts* phenotype
317 under these conditions.

318 Surprisingly, all the mutants grew more quickly than the control containing the
319 empty plasmid and similarly to WT. This suggests that these conserved amino acids are
320 not essential for rescuing the *ts* phenotype. However, it was difficult to distinguish
321 additional differences between yeast expressing WT or any of the Cwc15p mutants. One
322 possibility is that the *ts* phenotype arises from loss of Cwc15p interactions besides those
323 shown in **Fig. 5.** Cwc15 has not been fully resolved in any spliceosome structure from
324 any organism—the structural environment of large portions of the protein are unknown.
325 For example, in the most highly resolved spliceosome structure from *S. cerevisiae*, 58%
326 of the Cwc15p peptide could not be modeled (Senn et al. 2024). The *ts* phenotype could
327 depend on spliceosomal interactions not yet structurally defined or Cwc15p's interactions
328 with other machineries such as the transcription and export (TREX) complex (Henke-
329 Schulz et al. 2024).

330 <u>Genetic Interaction Between *CWC15* and Destabilizing U6 snRNA Mutants</u>

331 Finally, we further tested the idea that Cwc15p stabilizes the active site by
332 introducing destabilizing mutations into the U6 snRNA in regions that contact the N-
333 terminus of Cwc15p (**Fig. 6A**). We introduced U6 A62U, G63U, C84G, or C85G mutations
334 since it was previously shown that these U6 variants have little effect on yeast growth by
335 themselves (McPheeters 1996). When the growth of *CWC15* and *cwc15Δ* yeast were
336 compared with these variants, we observed a synthetic sick interaction between *cwc15*Δ
337 and the U6 snRNA A62U mutation at 37ºC. It is not obvious what structural explanation
338 could account for this. One possibility is that Cwc15p could prevent inappropriate wobble
339 pairing between U6 A62U and U2 nucleotides G20 or G21 in precatalytic or catalytic
340 spliceosomes (Senn et al. 2024; Galej et al. 2016; Rauhut et al. 2016). The conformation
341 of U2 G20 may be particularly important for proper active site formation (see **Sup. Fig.**
342 **S2** and Discussion). For the remaining U6 snRNA mutations studied here, it is likely that
343 they were not as significantly destabilizing and lack observable Cwc15p-dependent
344 phenotypes in these assays.

345 **DISCUSSION**

346 In summary, our data support a model in which Cwc15p fine-tunes the spliceosome
347 active site during 5'SS cleavage and also impacts transitions between spliceosome
348 conformations. The notion that non-essential *S. cerevisiae* splicing factors like Cwc15p
349 perturb catalytic conformations of the spliceosome or enforce fidelity has previously been
350 discussed with respect to other components of the NTC and the Ecm2 and Fyv6 proteins
351 (Hogg et al. 2010; Senn et al. 2024; Lipinski et al. 2023; van der Feltz et al. 2021). Our
352 group has previously proposed that non-essentiality may be linked to the relatively low
353 number of unique connections proteins like Cwc15p make between essential factors and

354 built-in interaction redundancy in the spliceosome (Kaur et al. 2022). Despite this, many
355 non-essential splicing factors become critical at low or high temperatures or in certain
356 genetic backgrounds. This could indicate that their conservation is due to subtle
357 modulation of the splicing machinery or the need for additional structural stability under
358 non-optimal growth conditions.

359 Beyond *S. cerevisiae*, this modulation may be critical for regulating alternative
360 splicing and result in Cwc15 essentiality. One aspect of this model is potential adaptation
361 (or exploitation) of Cwc15 for changing splicing outcomes in response to cellular
362 conditions. For example, direct interaction between the *P. infestans* virulence protein IPI-
363 O1 and the potato host protein StCwc15 leads to relocalization of StCwc15 from the
364 nucleoplasm to the nucleolus and nuclear speckles (Sun et al. 2024). This interaction also
365 results in a change in splicing of the *RB* immunity gene pre-mRNA leading to a decrease
366 in the intron-retained isoform and an increase in the fully-spliced mRNA (Sun et al. 2024).
367 While the molecular mechanism for this switch has not yet been determined, other NTC
368 components are also subject to dynamic regulation including by post-translational
369 modification (Lu and Legerski 2007; Lleres et al. 2010; de Almeida and O'Keefe 2015).
370 This provides a plausible mechanism by which external factors could modulate Cwc15's
371 activity and, consequently, 5'SS cleavage efficiency.

372 Determining a more precise role for Cwc15p during splicing is challenging, and the
373 data are most consistent with the protein functioning in stabilizing the 1st-step active site
374 during structural transitions as well as during catalysis. Yeast with Cwc15p show
375 increased tolerance to Cu^{2+} using ACT1-CUP1 splicing reporters harboring a 5'SS U2C
376 substitution and several BS substitutions (**Fig. 4**). Additionally, loss of Cwc15p

377 suppresses growth defects associated with Prp8p 1st-step alleles (**Fig. 3**) and results in a
378 growth defect in the presence of a likely destabilizing U6 snRNA mutation (**Fig. 6**). These
379 data not only suggest that Cwc15p stabilizes the 1st-step conformation of the spliceosome
380 but that this may also be particularly important when non-consensus substrates or mutant
381 splicing factors are present.

382 Among our results, genetic interactions between *cwc15*Δ and Prp2p^{Q5548N} and U6-
383 U57C mutations are particularly interesting. In both cases, the *CWC15* deletion has a
384 negative genetic interaction with these mutations. While interpretation of U6 U57C
385 mutations can be complex (Wlodaver and Staley 2014; McPheeters 1996; Query and
386 Konarska 2004; Liu et al. 2007; Eysmont et al. 2019), the data are consistent with Cwc15p
387 also facilitating structural transitions into and out of the 1st-step active site conformation.
388 How exactly this occurs is unclear but could involve directly destabilizing the RNA
389 structures that form the spliceosome active site, stabilizing transient active site
390 conformations, or favoring formation of the stable products of these transitions. The latter
391 possibility would provide a parsimonious explanation for some of our results: stabilization
392 of the 1st-step active site by Cwc15p facilitates both its formation by Prp2 and 5'SS
393 cleavage itself.

394 An intriguing possibility is that Cwc15's conserved N-terminus participates in the
395 above processes directly. Analysis of multiple cryo-EM structures of *S. cerevisiae*
396 spliceosomes reveals that the very N-terminus of Cwc15p is located in between the U2
397 and U6 snRNAs in the B* spliceosome (the stage immediately preceding 5'SS cleavage)
398 and in this same position in subsequently formed complexes (B*→C→C*→P→ILS
399 complex spliceosomes) (Senn et al. 2024; Wan et al. 2017; Fica et al. 2017; Wan et al.

400 2019; Wilkinson et al. 2021) (**Fig. S2**). Importantly, in activated spliceosomes (B^{act})
401 trapped prior to Prp2p activity and formation of B*, this same region of Cwc15p could not
402 be modeled between the snRNAs and does not adopt a specific, stable conformation (see
403 **Fig. S2**) (Bai et al. 2021). Further, the N-terminus of Cwc15 proteins could not be modeled
404 in structures of an off-pathway, B^{act}-like *S. cerevisiae* spliceosome assembled on an
405 excised intron (Li et al. 2026) (Max Wilkinson, personal communication); a human
406 spliceosome trapped while Prp2 was functioning (Schmitzova et al. 2023); or in *S. pombe*
407 and *Chaetomium thermophilum* spliceosomes trapped prior to the B* stage and in the
408 midst of being disrupted by the DHX35 ATPase (Soni et al. 2025; Li et al. 2025). Stable
409 insertion of the Cwc15 N-terminus in between the U2 and U6 snRNAs may be a
410 consequence of Prp2 activity and a marker of a correctly assembled active site.
411 Conversely, a dynamic Cwc15 N-terminus (or just lack of its insertion between U2 and
412 U6) may facilitate active site disruption and proofreading by DHX35. These putative
413 functions are evidently not essential in *S. cerevisiae* (see **Figs. 1, 5**), in which a
414 corresponding DHX35-like activity has also not yet been identified.

415 The involvement of Cwc15p in other steps in gene expression besides pre-mRNA
416 splicing complicates phenotypic analysis in our assays. In addition to splicing, Cwc15p is
417 also important for tethering the TREX complex to the NTC, which itself is involved in both
418 pre-mRNA splicing and transcription elongation (Henke-Schulz et al. 2024; Chanarat et
419 al. 2011). Further, loss of *CWC15* has a negative genetic interaction with deletion of the
420 general transcription factor TFIIS (*dst1*Δ) (Henke-Schulz et al. 2024). Given the high
421 degree of coupling between transcription and splicing (Carrocci and Neugebauer 2024),
422 it is likely that the growth phenotypes reported here have contributions from both

423 processes. Future deconvolution of Cwc15p function may benefit from both molecular
424 and genetic approaches to disentangle these processes as well as studies in model
425 organisms in which the protein is essential for viability.

426 **DATA AND REAGENT AVAILABILITY**

427 Strains and plasmids are available upon request. The authors affirm that all data
428 necessary for confirming the conclusions of the article are present within the article,
429 figures, and tables.

430 **ACKNOWLEDGMENTS**

431 We thank Joshua Paulson for help in preparation of microbial growth media. We
432 thank Laura Vanderploeg for help with figures. We thank Max Wilkinson (Memorial Sloan
433 Kettering Cancer Center) for helpful discussions about the structure of Cwc15 and for
434 making figures S2A and B.

435 **AUTHOR CONTRIBUTIONS**

436 NZ, DH, AAH: project conceptualization; NZ, ZF, AAH: media and reagent
437 preparation; NZ, GB, ZF, SJ, and AAH: data acquisition and analysis; DH, AAH: writing
438 and editing of the manuscript with input from NZ.

439 **STUDY FUNDING**

440 This work was supported by a grant from the USDA (HATCH WIS06060). Funding
441 for DH was provided by USDA-ARS CRIS 5090-21220-005-00D. Funding for SJ was
442 provided by the University of Wisconsin-Madison Summer Research Opportunities
443 Program.

444

445 **CONFLICT OF INTEREST**

446 AAH is carrying out sponsored research for Remix Therapeutics.

447

448 **REFERENCES**

449 Bai, R., R. Wan, C. Yan, Q. Jia, J. Lei *et al.*, 2021 Mechanism of spliceosome remodeling by the
450 ATPase/helicase Prp2 and its coactivator Spp2. *Science* 371 (6525).

451 Carrocci, T.J., and K.M. Neugebauer, 2024 Emerging and re-emerging themes in co-transcriptional pre-
452 mRNA splicing. *Mol Cell* 84 (19):3656–3666.

453 Carrocci, T.J., J.C. Paulson, and A.A. Hoskins, 2018 Functional analysis of Hsh155/SF3b1 interactions
454 with the U2 snRNA/branch site duplex. *RNA* 24 (8):1028–1040.

455 Carrocci, T.J., D.M. Zoerner, J.C. Paulson, and A.A. Hoskins, 2017 SF3b1 mutations associated with
456 myelodysplastic syndromes alter the fidelity of branchsite selection in yeast. *Nucleic Acids Res* 45
457 (8):4837–4852.

458 Chanarat, S., M. Seizl, and K. Strasser, 2011 The Prp19 complex is a novel transcription elongation factor
459 required for TREX occupancy at transcribed genes. *Genes Dev* 25 (11):1147–1158.

460 Chung, C.S., C.K. Tseng, H.C. Chen, and S.C. Cheng, 2025 New mechanistic insights into Prp22-
461 mediated exon ligation and mRNA release. *Nucleic Acids Res* 53 (16).

462 Chung, C.S., H.L. Wai, C.Y. Kao, and S.C. Cheng, 2023 An ATP-independent role for Prp16 in promoting
463 aberrant splicing. *Nucleic Acids Res* 51 (20):10815–10828.

464 Company, M., J. Arenas, and J. Abelson, 1991 Requirement of the RNA helicase-like protein PRP22 for
465 release of messenger RNA from spliceosomes. *Nature* 349 (6309):487–493.

466 de Almeida, R.A., and R.T. O'Keefe, 2015 The NineTeen Complex (NTC) and NTC-associated proteins as
467 targets for spliceosomal ATPase action during pre-mRNA splicing. *RNA Biol* 12 (2):109–114.

468 Eysmont, K., K. Matylla-Kulinska, A. Jaskulska, M. Magnus, and M.M. Konarska, 2019 Rearrangements
469 within the U6 snRNA Core during the Transition between the Two Catalytic Steps of Splicing. *Mol*
470 *Cell* 75 (3):538–548 e533.

471 Fica, S.M., C. Oubridge, W.P. Galej, M.E. Wilkinson, X.C. Bai *et al.*, 2017 Structure of a spliceosome
472 remodelled for exon ligation. *Nature* 542 (7641):377–380.

473 Fica, S.M., N. Tuttle, T. Novak, N.S. Li, J. Lu *et al.*, 2013 RNA catalyses nuclear pre-mRNA splicing.
474 *Nature* 503 (7475):229–234.

475 Galej, W.P., M.E. Wilkinson, S.M. Fica, C. Oubridge, A.J. Newman *et al.*, 2016 Cryo-EM structure of the
476 spliceosome immediately after branching. *Nature* 537 (7619):197–201.

477 Goldstein, A.L., and J.H. McCusker, 1999 Three new dominant drug resistance cassettes for gene
478 disruption in Saccharomyces cerevisiae. *Yeast* 15 (14):1541–1553.

479 Grainger, R.J., and J.D. Beggs, 2005 Prp8 protein: at the heart of the spliceosome. *RNA* 11 (5):533–557.

480 Guthrie, C., G.R. Fink, J.N. Abelson, M.I. Simon, and ScienceDirect, 1991 *Guide to yeast genetics and*
481 *molecular biology*. San Diego ; London: Academic Press.

482 Henke-Schulz, L., R. Minocha, N.H. Maier, and K. Strasser, 2024 The Prp19C/NTC subunit Syf2 and the
483 Prp19C/NTC-associated protein Cwc15 function in TREX occupancy and transcription elongation.
484 *RNA* 30 (7):854–865.

485 Hogg, R., J.C. McGrail, and R.T. O'Keefe, 2010 The function of the NineTeen Complex (NTC) in
486 regulating spliceosome conformations and fidelity during pre-mRNA splicing. *Biochem Soc Trans*
487 38 (4):1110–1115.

488 Hotz, H.R., and B. Schwer, 1998 Mutational analysis of the yeast DEAH-box splicing factor Prp16.
489 *Genetics* 149 (2):807–815.

490 Hoyos-Manchado, R., F. Reyes-Martin, C. Rallis, E. Gamero-Estevez, P. Rodriguez-Gomez *et al.*, 2017
491 RNA metabolism is the primary target of formamide in vivo. *Sci Rep* 7 (1):15895.

492 Kastner, B., C.L. Will, H. Stark, and R. Lührmann, 2019 Structural Insights into Nuclear pre-mRNA
493 Splicing in Higher Eukaryotes. *Cold Spring Harb Perspect Biol* 11 (11).

494 Kaur, H., C. van der Feltz, Y. Sun, and A.A. Hoskins, 2022 Network theory reveals principles of
495 spliceosome structure and dynamics. *Structure* 30 (1):190–200 e192.

496 Koodathingal, P., T. Novak, J.A. Piccirilli, and J.P. Staley, 2010 The DEAH box ATPases Prp16 and Prp43
497 cooperate to proofread 5' splice site cleavage during pre-mRNA splicing. *Mol Cell* 39 (3):385–
498 395.

499 Lardelli, R.M., J.X. Thompson, J.R. Yates, 3rd, and S.W. Stevens, 2010 Release of SF3 from the intron
500 branchpoint activates the first step of pre-mRNA splicing. *RNA* 16 (3):516–528.

501 Lesser, C.F., and C. Guthrie, 1993 Mutational analysis of pre-mRNA splicing in Saccharomyces cerevisiae
502 using a sensitive new reporter gene, CUP1. *Genetics* 133 (4):851–863.

503 Li, G.W., M.E. Wilkinson, and D.P. Bartel, 2026 The spliceosome assembles on excised linear introns to
504 protect them from degradation. *bioRxiv*:2026.2001.2021.700889.

505 Li, Y., P. Fischer, M. Wang, Q. Zhou, A. Song *et al.*, 2025 Structural insights into spliceosome fidelity:
506 DHX35-GPATCH1- mediated rejection of aberrant splicing substrates. *Cell Res* 35 (4):296–308.

507 Lipinski, K.A., K.A. Senn, N.J. Zeps, and A.A. Hoskins, 2023 Biochemical and genetic evidence supports
508 Fyv6 as a second-step splicing factor in Saccharomyces cerevisiae. *RNA* 29 (11):1792–1802.

509 Liu, L., C.C. Query, and M.M. Konarska, 2007 Opposing classes of prp8 alleles modulate the transition
510 between the catalytic steps of pre-mRNA splicing. *Nat Struct Mol Biol* 14 (6):519–526.

511 Lleres, D., M. Denegri, M. Biggiogera, P. Ajuh, and A.I. Lamond, 2010 Direct interaction between hnRNP-
512 M and CDC5L/PLRG1 proteins affects alternative splice site choice. *EMBO Rep* 11 (6):445–451.

513 Lu, X., and R.J. Legerski, 2007 The Prp19/Pso4 core complex undergoes ubiquitylation and structural
514 alterations in response to DNA damage. *Biochem Biophys Res Commun* 354 (4):968–974.

515 Mayas, R.M., H. Maita, and J.P. Staley, 2006 Exon ligation is proofread by the DExD/H-box ATPase
516 Prp22p. *Nat Struct Mol Biol* 13 (6):482–490.

517 McPheeters, D.S., 1996 Interactions of the yeast U6 RNA with the pre-mRNA branch site. *RNA* 2
518 (11):1110–1123.

519 Meng, E.C., T.D. Goddard, E.F. Pettersen, G.S. Couch, Z.J. Pearson *et al.*, 2023 UCSF ChimeraX: Tools
520 for structure building and analysis. *Protein Sci* 32 (11):e4792.

521 Ohi, M.D., A.J. Link, L. Ren, J.L. Jennings, W.H. McDonald *et al.*, 2002 Proteomics analysis reveals
522 stable multiprotein complexes in both fission and budding yeasts containing Myb-related
523 Cdc5p/Cef1p, novel pre-mRNA splicing factors, and snRNAs. *Mol Cell Biol* 22 (7):2011–2024.

524 Plaschka, C., A.J. Newman, and K. Nagai, 2019 Structural Basis of Nuclear pre-mRNA Splicing: Lessons
525 from Yeast. *Cold Spring Harb Perspect Biol* 11 (5).

526 Query, C.C., and M.M. Konarska, 2004 Suppression of multiple substrate mutations by spliceosomal prp8
527 alleles suggests functional correlations with ribosomal ambiguity mutants. *Mol Cell* 14 (3):343–
528 354.

529 Query, C.C., and M.M. Konarska, 2012 CEF1/CDC5 alleles modulate transitions between catalytic
530 conformations of the spliceosome. *RNA* 18 (5):1001–1013.

531 Rauhut, R., P. Fabrizio, O. Dybkov, K. Hartmuth, V. Pena *et al.*, 2016 Molecular architecture of the
532 Saccharomyces cerevisiae activated spliceosome. *Science* 353 (6306):1399–1405.

533 Sales-Lee, J., D.S. Perry, B.A. Bowser, J.K. Diedrich, B. Rao *et al.*, 2021 Coupling of spliceosome
534 complexity to intron diversity. *Curr Biol* 31 (22):4898–4910 e4894.

535 Schmitzova, J., C. Cretu, C. Dienemann, H. Urlaub, and V. Pena, 2023 Structural basis of catalytic
536 activation in human splicing. *Nature* 617 (7962):842–850.

537 Schwer, B., and T. Meszaros, 2000 RNA helicase dynamics in pre-mRNA splicing. *EMBO J* 19 (23):6582–
538 6591.

539 Senn, K.A., K.A. Lipinski, N.J. Zeps, A.F. Griffin, M.E. Wilkinson *et al.*, 2024 Control of 3' splice site
540 selection by the yeast splicing factor Fyv6. *Elife* 13.

541 Silva, D., G. Santos, M. Barroca, D. Costa, and T. Collins, 2023 Inverse PCR for Site-Directed
542 Mutagenesis. *Methods Mol Biol* 2967:223–238.

543 Slane, D., C.H. Lee, M. Kolb, C. Dent, Y. Miao *et al.*, 2020 The integral spliceosomal component CWC15
544 is required for development in Arabidopsis. *Sci Rep* 10 (1):13336.

545 Soni, K., A. Horvath, O. Dybkov, M. Schwan, S. Trakansuebkul *et al.*, 2025 Structures of aberrant
546 spliceosome intermediates on their way to disassembly. *Nat Struct Mol Biol* 32 (5):914–925.

547 Sonstegard, T.S., J.B. Cole, P.M. VanRaden, C.P. Van Tassell, D.J. Null *et al.*, 2013 Identification of a
548 nonsense mutation in CWC15 associated with decreased reproductive efficiency in Jersey cattle.
549 *PLoS One* 8 (1):e54872.

550 Sun, B., J. Huang, L. Kong, C. Gao, F. Zhao *et al.*, 2024 Alternative splicing of a potato disease
551 resistance gene maintains homeostasis between growth and immunity. *Plant Cell* 36 (9):3729–
552 3750.

553 Tseng, C.K., H.L. Liu, and S.C. Cheng, 2011 DEAH-box ATPase Prp16 has dual roles in remodeling of the
554 spliceosome in catalytic steps. *RNA* 17 (1):145–154.

555 van der Feltz, C., B. Nikolai, C. Schneider, J.C. Paulson, X. Fu *et al.*, 2021 Saccharomyces cerevisiae
556 Ecm2 modulates the catalytic steps of pre-mRNA splicing. *RNA* 27 (5):591–603.

557 Wan, R., R. Bai, C. Yan, J. Lei, and Y. Shi, 2019 Structures of the Catalytically Activated Yeast
558 Spliceosome Reveal the Mechanism of Branching. *Cell* 177 (2):339–351 e313.

559 Wan, R., C. Yan, R. Bai, J. Lei, and Y. Shi, 2017 Structure of an Intron Lariat Spliceosome from
560 Saccharomyces cerevisiae. *Cell* 171 (1):120–132 e112.

561 Wilkinson, M.E., S.M. Fica, W.P. Galej, and K. Nagai, 2021 Structural basis for conformational equilibrium
562 of the catalytic spliceosome. *Mol Cell* 81 (7):1439–1452 e1439.

563 Wlodaver, A.M., and J.P. Staley, 2014 The DExD/H-box ATPase Prp2p destabilizes and proofreads the
564 catalytic RNA core of the spliceosome. *RNA* 20 (3):282–294.

565 Yan, C., R. Wan, and Y. Shi, 2019 Molecular Mechanisms of pre-mRNA Splicing through Structural
566 Biology of the Spliceosome. *Cold Spring Harb Perspect Biol* 11 (1).
567
568

FIGURES AND FIGURE LEGENDS

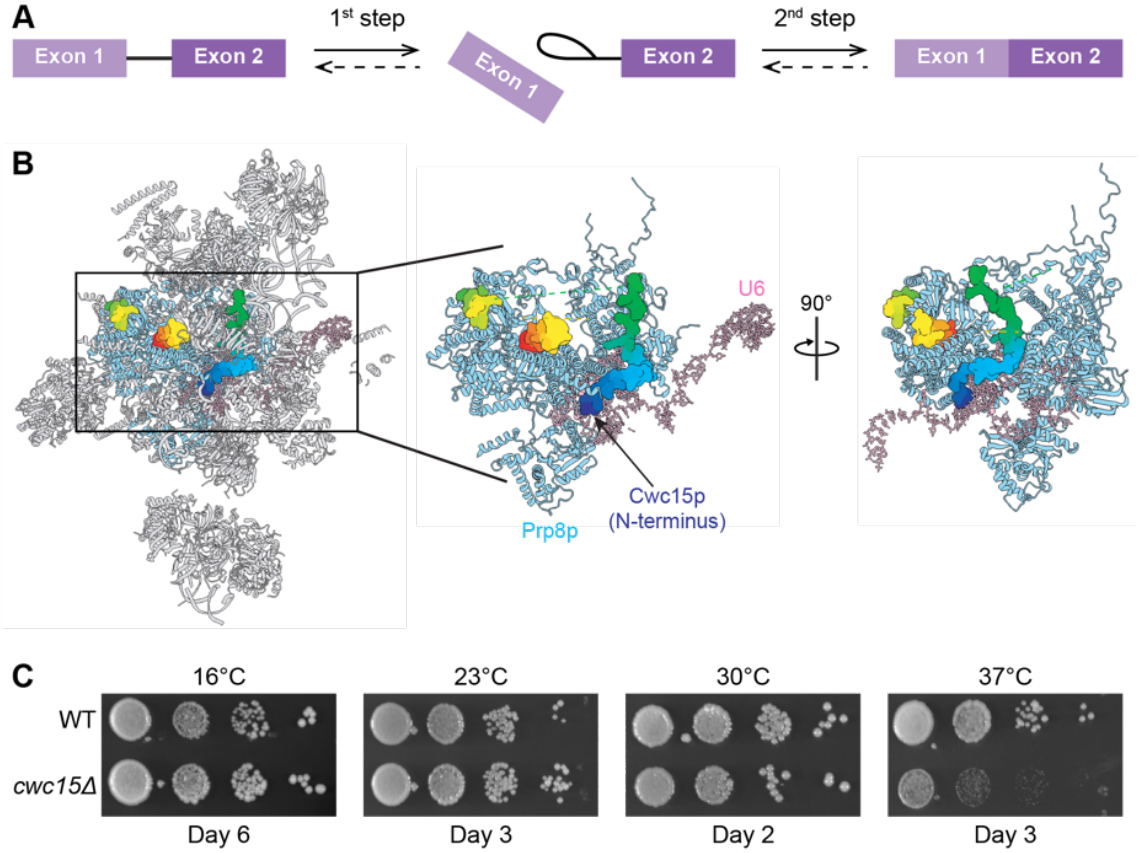

Figure 1. The transesterification steps in pre-mRNA splicing and location of Cwc15p in the spliceosome. (**A**) The two transesterification steps in splicing involve 5'SS cleavage (1st step) and exon ligation (2nd step). (**B**) Location of Cwc15p in the *S. cerevisiae* product (P) complex spliceosome (PDB 9DTR). This view shows the spliceosome in grey cartoon representation with Cwc15p shown in spacefill and colored with a gradient from blue (N-terminus) to red (C-terminus). Not all of the Cwc15p peptide chain could be modeled in the structure. Prp8p and U6 snRNA are also shown in blue and pink, respectively. A clipping mask was used to make the spliceosome active site and Cwc15p more visible. This figure was generated using ChimeraX (Meng et al. 2023). (**C**)Yeast without *CWC15* exhibit a *ts* phenotype at 37°C. For panel C, yeast were grown on YPD plates and imaged after the given number of days.

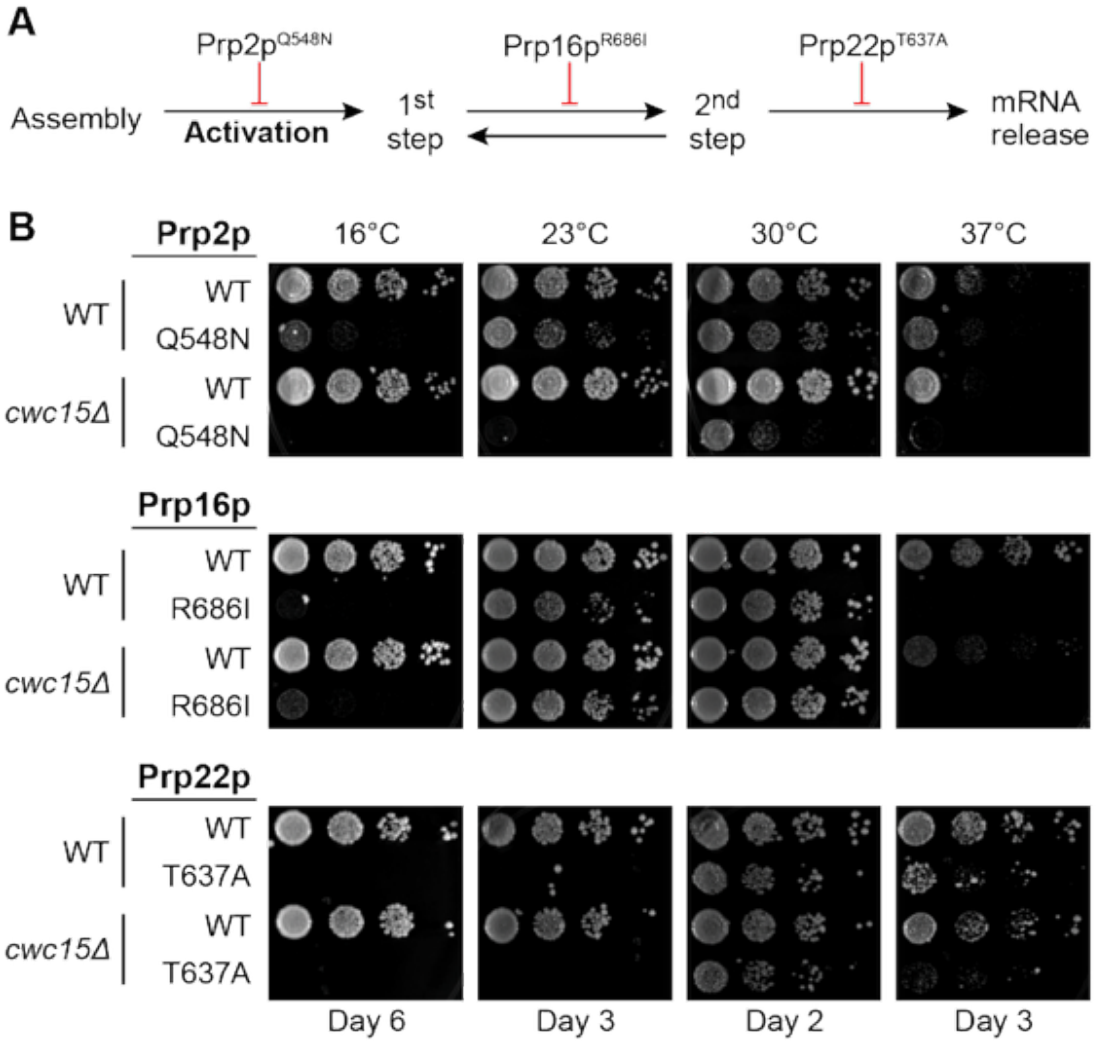

Figure 2. Genetic interactions between *CWC15* and spliceosome DEAH-box ATPases. (**A**) Schematic showing spliceosome remodeling events promoted by Prp2p, Prp16p, and Prp22p which promote activation, the 1st-to-2nd step transition, and mRNA release, respectively. The mutations shown can inhibit these transitions and also impact pre-mRNA splicing fidelity. (**B**) Deletion of *CWC15* causes a negative genetic interaction with Prp2p^{Q548N}. Genetic interactions with Prp16p and Prp22p mutants were less apparent, although weak suppression of the Prp16p^{R686I} could be observed at 16 and 23°C and Prp22p^{T637A} strengthened the *ts* phenotype caused by *cwc15Δ* at 37°C. For panel B, yeast were grown on YPD plates and imaged after the given number of days.

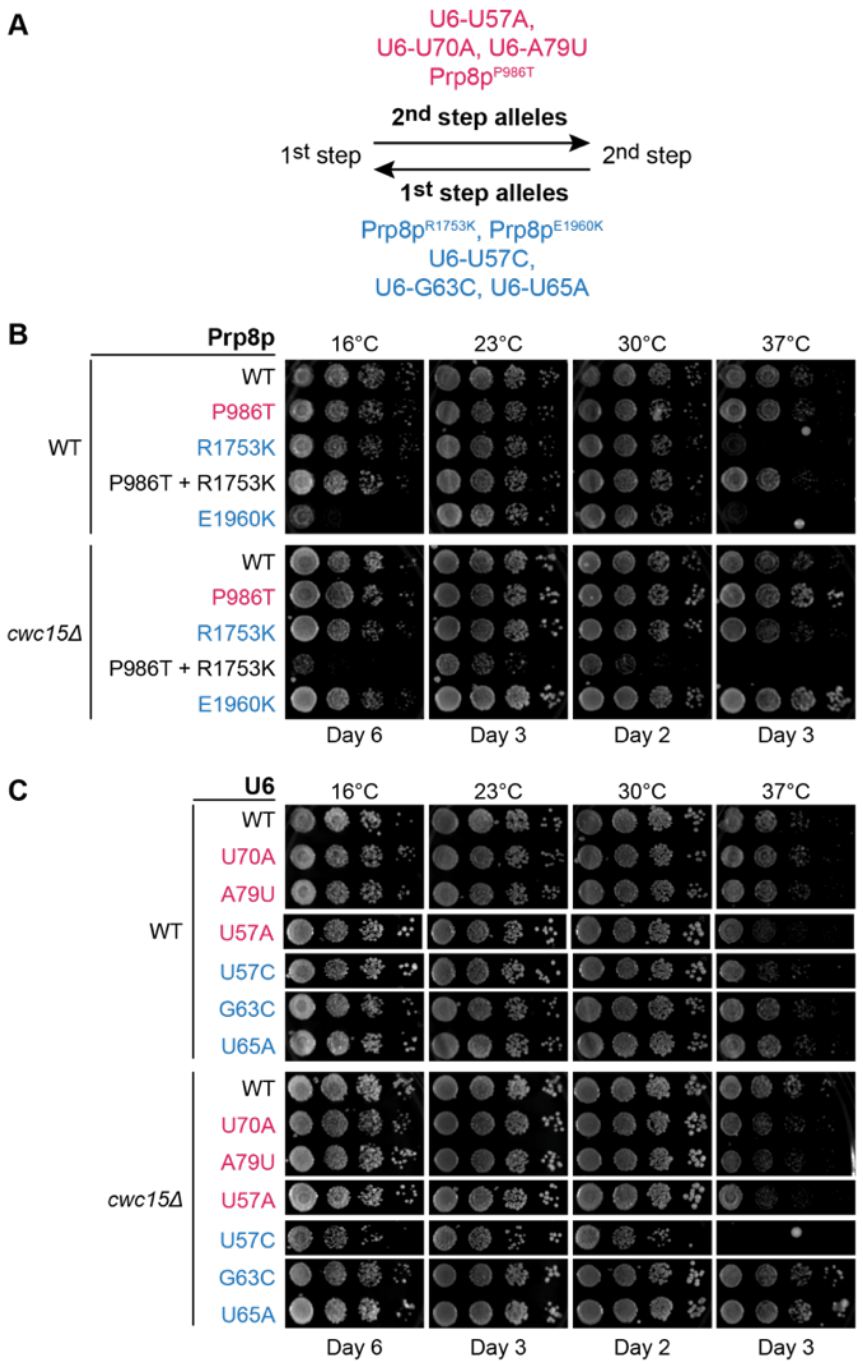

Figure 3. Genetic interactions between *CWC15* and *PRP8* or *SNR6* (U6 snRNA). (**A**) 1st-step alleles (blue) of Prp8p or U6 snRNA promote 5'SS cleavage and the 1st-step configuration of the spliceosome at the expense of the 2nd step. 2nd-step alleles do the opposite (red). (**B**) Loss of *CWC15* can rescue the *ts* phenotype caused by Prp8 1st-step alleles. (**C**) Loss of *CWC15* is synthetic lethal with U6-U57C (1st-step allele) at 37°C and causes a *cs* phenotype at 16°C. For panels B and C, yeast were grown on YPD plates and imaged after the given number of days.

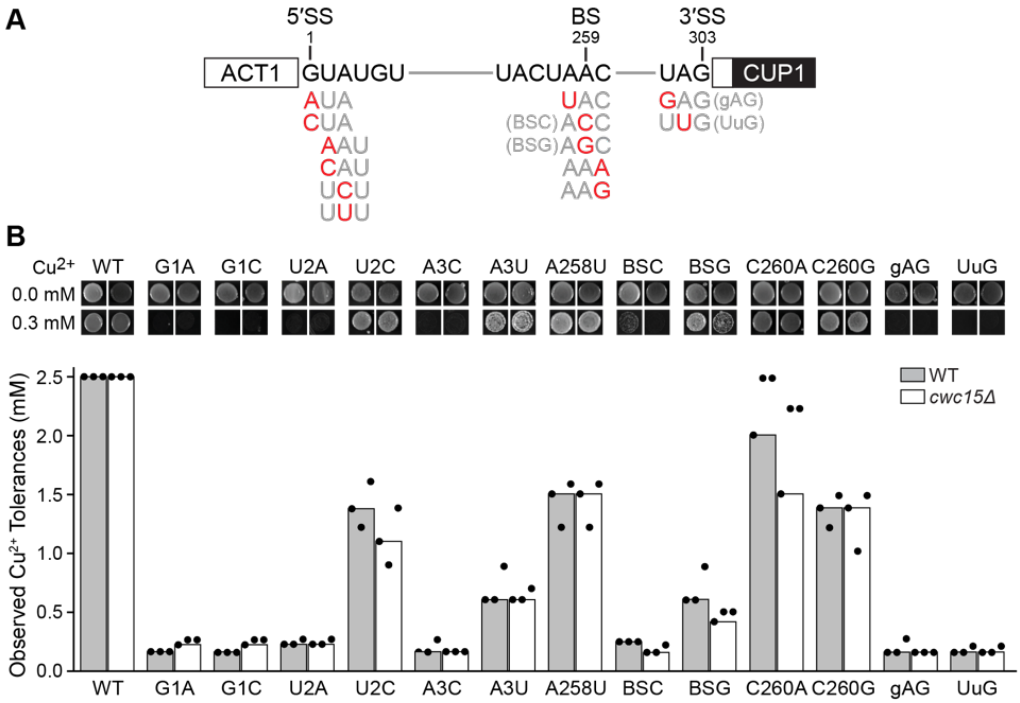

Figure 4. Loss of Cwc15p impacts Cu^{2+} tolerances of yeast expressing non-consensus ACT1-CUP1 reporters. (**A**) Schematic of the ACT1-CUP1 reporter pre-mRNA with the tested substitutions shown. (**B**) Loss of Cwc15p changes copper tolerances for yeast expressing reporter pre-mRNAs with particular substitutions within the 5'SS or BS but not for those expressing a reporter with consensus sites (WT). Bar heights represent values obtained from a single replicate of the ACT1-CUP1 assay. Dots represent values obtained for all three replicates. Yeast were grown at 30ºC on -Leu DO plates containing various [Cu^{2+}] and imaged after 3 days.

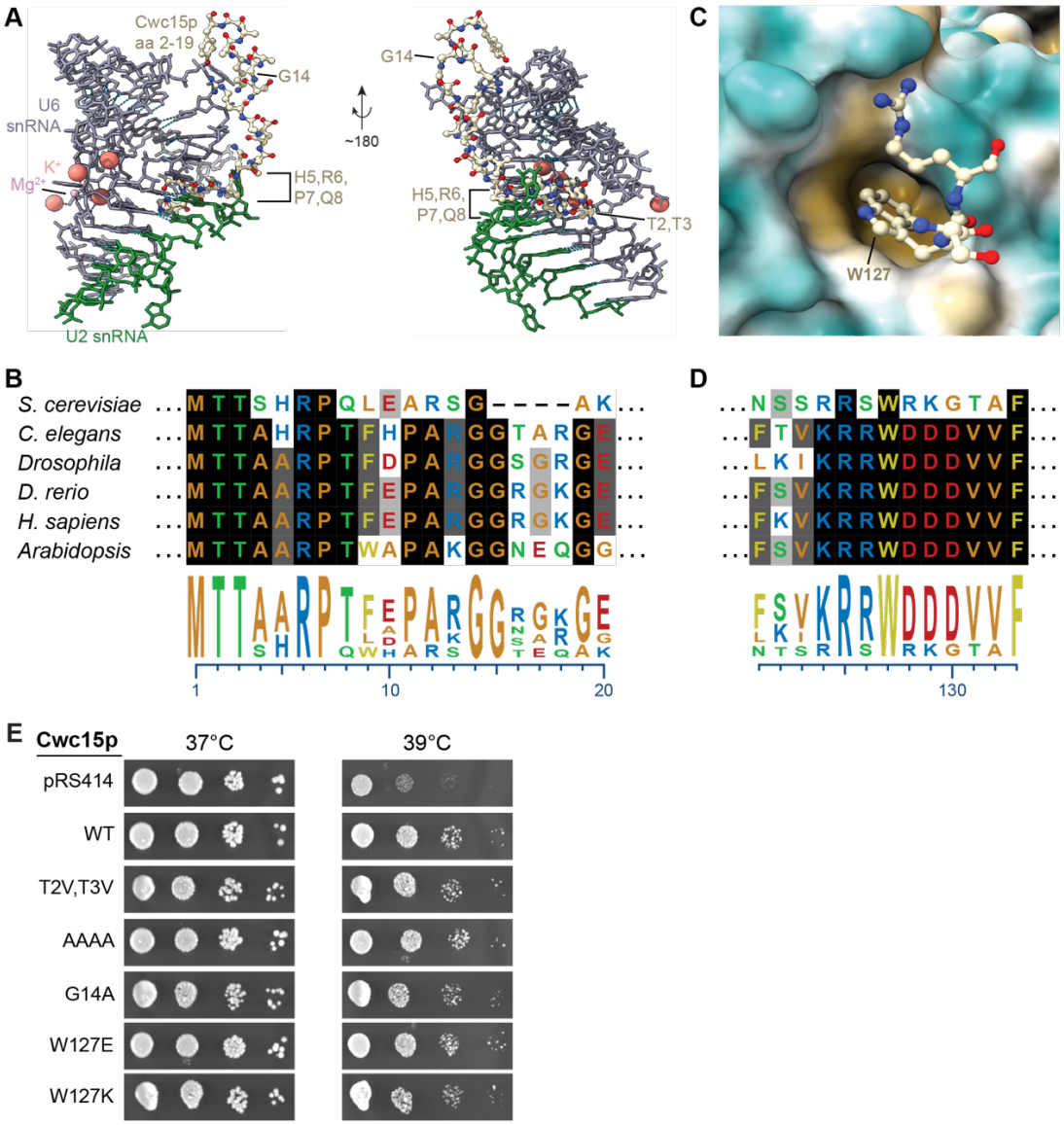

Figure 5. Cwc15p mutants can complement a *cwc15*Δ growth defect. (**A**) Close-up of Cwc15p N-terminus interactions with the U2/U6 di-snRNA within the active site of a P complex spliceosome (PDB 9DTR). The active site can be identified by the presence of Mg^{2+} and K^{+} ions. (**B**) Sequence alignments and logos for Cwc15 from single and multicellular model organisms and humans. The N-terminus of Cwc15 is highly conserved among eukaryotes. (**C**) Close-up of the interaction of Cwc15p residue Trp127 with a hydrophobic pocket on Prp8p (surface representation, hydrophobic surfaces shown in yellow and hydrophilic in blue-green). (**D**) Trp127 is also highly conserved. (**E**) Growth assays of *cwc15*Δ yeast expressing Cwc15p mutants relative to WT and empty plasmid (pRS414) controls. Yeast were grown on -TRP DO plates and imaged after 2 days. Panels A and C were created using ChimeraX (Meng et al. 2023). Sequence alignments and logos for panels B and D were generated using MegAlign Pro (Lasergene, DNASTAR, Inc.).

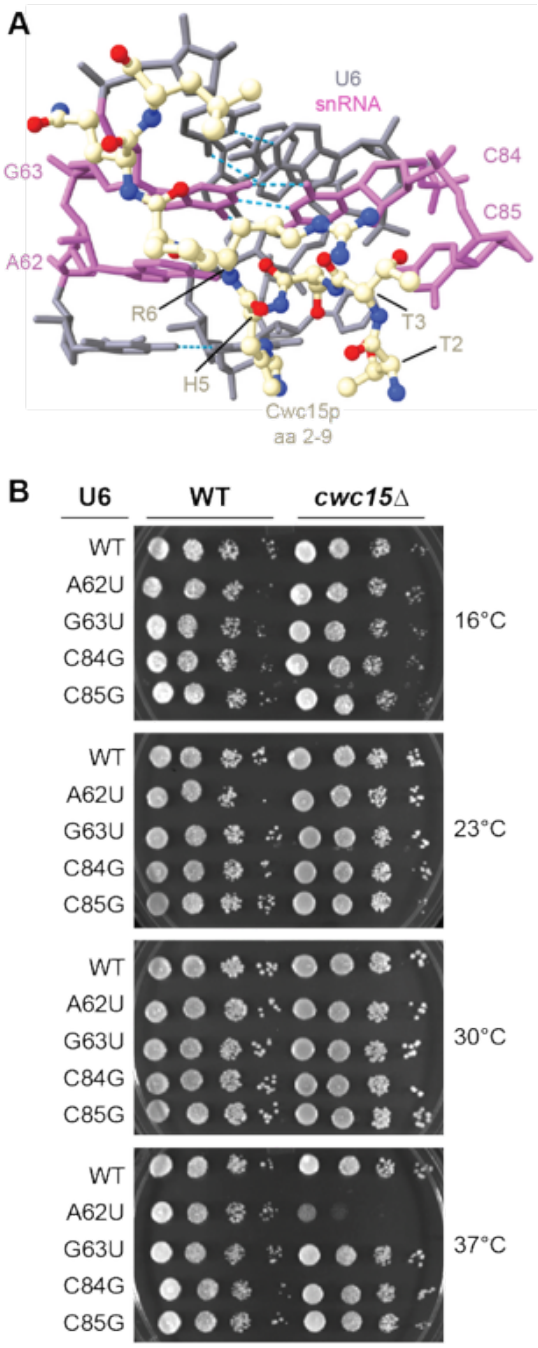

Figure 6. Genetic interactions between potentially active site-destabilizing mutations in the U6 snRNA and *CWC15*. A negative genetic interaction is observed between U6 snRNA A62U and *cwc15*Δ at 37oC. Yeast were grown on YPD plates and imaged after 2 (30ºC), 3 (23 and 37ºC), or 6 days (16ºC). Panel A was created using ChimeraX (Meng et al. 2023).